Anal. Chem. **2005,** *77,* 4390−4397

Identification of Single Bacterial Cells in Aqueous Solution Using Confocal Laser Tweezers Raman Spectroscopy

C. Xie,[†] J. Mace,[†] M. A. Dinno,[†] Y. Q. Li,*[,†] W. Tang,[‡] R. J. Newton,[‡] and P. J. Gemperline[§]

Departments of Physics, Biology, and Chemistry, East Carolina University, Greenville, North Carolina 27858-4353

We report on a rapid method for reagentless identification and discrimination of single bacterial cells in aqueous solutions using a combination of laser tweezers and confocal Raman spectroscopy (LTRS). The optical trapping enables capturing of individual bacteria in aqueous solution in the focus of the laser beam and levitating the captured cell well off the cover plate, thus maximizing the excitation and collection of Raman scattering from the cell and minimizing the unwanted background from the cover plate and environment. Raman spectral patterns excited by a near-infrared laser beam provide intrinsic molecular information for reageatless analysis of the optically isolated bacterium. In our experiments, six species of bacteria were used to demonstrate the capability of the confocal LTRS in the identification and discrimination between the diverse bacterial species at various growth conditions. We show that synchronized bacterial cells can be well-discriminated among the six species using principal component analyses (PCA). Unsynchronized bacterial cells that are cultured at stationary phases can also be well-discriminated by the PCA, as well as by a hierarchical cluster analysis (HCA) of their Raman spectra. We also show that unsynchronized bacteria selected from random growth phases can be classified with the help of a generalized discriminant analysis (GDA). These findings demonstrate that the LTRS may find valuable applications in rapid sensing of microbial cells in diverse aqueous media.

The ability to rapidly and accurately identify and ascertain the species of potent pathogens is still a challenge for environmentalists and microbiologists. The presumptive identification of bacteria begins with inspecting the colony morphology. Upon the morphological characteristics, a series of tests are performed to examine the biochemical, physiological, and nutritional properties of a microorganism so as to get confirmatory identification.[1,2] With these traditional methods, a significant incubation period is generally required to get a large biomass before pure culture tests are performed, which significantly reduces the effectiveness of cultured-based methods for rapid microbial analysis. And more, in many circumstances, some microorganisms in the environment cannot be cultured under laboratory conditions. These demand the development of new sensing techniques that work within minutes or without laboratory bacterial incubation.

In recent years, much effort has been invested in the development of new techniques for the identification of microorganisms, which include molecular methods, such as PCR and in situ hybridization,[3,4] mass spectrometry,[5] electrospray ionization and matrix-assisted laser desorption ionization,[6] FT-IR spectroscopy,[2,7] and Raman spectroscopy.[8−11] Among these methods, vibrational spectroscopy (FT-IR and Raman) is a reagentless procedure in which there is no need to add chemical dyes or labels for identification. The characteristics of the absorbed or scattered light depend on the molecules found within the sample and the environment in which the molecules are found. Another advantage of vibrational spectroscopy is that it is a rapid, specific, and noninvasive analytical method which provides a promising means for the identification of a single bacterium. When compared to FT-IR, which is for measuring the IR absorption of the sample, Raman spectroscopy measures the inelastically scattered light following excitation. The advantages of Raman spectroscopy are that for aqueous samples, the IR absorption of water is avoided and spectral bands are more sharp and distinguishable. Biological molecules such as nucleic acids, protein, lipids, and carbohydrates all generate specific Raman spectra, which provide biochemical information regarding the molecular composition, structure, and interactions in cells. The molecular composition and structure are different among different bacterial species. Therefore, from the

* Corresponding author. Fax: 252-328-6314. E-mail: liy@mail.ecu.edu.
[†] Department of Physics.
[‡] Department of Biology.
[§] Department of Chemistry.

(1) Vanderberg, L. A. *Appl. Spectrosc.* **2000**, *54*, 376A−385A.
(2) Maquelin, K.; Kirschner, C.; Choo-Smith, L.-P.; van den Braak, N.; Endtz, H. Ph.; Naumann, D.; Puppels, G. J. *J. Microbiol. Methods* **2002**, *51*, 255−271.
(3) Belgrader, P.; Benett, W.; Hadley, D.; Richards, J.; Stratton, P.; Mariella, R.; Milanovich, F. *Science* **1999**, *284*, 449−450.
(4) Hamels, S.; Gala, J. L.; Dufour, S.; Vannuffel, P.; Zammatteo, N.; Remacle, J. *Biotechniques* **2001**, *31*, 1364−1372.
(5) Gikunju, C. M.; Lev, S. M.; Birenzvige, A.; Schaefer, M. D. *Talanta* **2004**, *62*, 741−744.
(6) Goodacre, R.; Heald, J. K.; Kell, D. B. *FEMS. Microbiol. Lett.* **1999**, *176*, 17−24.
(7) Franck, P.; Nabet, P.; Dousset, B. *Cell. Mol. Biol.* **1998**, *44*, 273−275.
(8) Maquelin, K.; Choo-Smith, L.-P.; van Vreeswijk, T.; Endtz, H. P.; Smith, B.; Bennett, R.; Bruining, H. A.; Puppels, G. J. *Anal. Chem.* **2000**, *72*, 12−19.
(9) Maquelin, K.; Choo-Smith, L.-P.; Endtz, H. P.; Bruining, H. A.; Puppels, G. J. *J. Clin. Microbiol.* **2002**, *40*, 594−600.
(10) Huang, W. E.; Griffiths, R. I.; Thompson, I. P.; Bailey, M. J.; Whiteley, A. S. *Anal. Chem.* **2004**, *76*, 4452−4458.
(11) Perty, R.; Schmitt, M.; Popp, J. *ChemPhysChem* **2003**, *14*, 14−30.

10.1021/ac0504971 CCC: $30.25
Published on Web 05/28/2005

whole-cell spectra, single microorganisms could be identified and discriminated.[8,9]

Most recently, Raman microscopy has been coupled with confocal light collection,[9,12] which defines a small excitation/collection volume for probing local structures by imaging the collected scattering through a small pinhole. The Raman signal from only the focal region of the objective is collected, while the background signals that are out of the focus are rejected. The high spatial resolution provided by confocal Raman microscopy enables detection of both the spectral features of single cells and interior organelles. In Raman microscopy, the targeted cells must be immobilized by physical or chemical contact.

Another exciting development of Raman spectroscopy is combination with optical tweezers for the analysis of moving cells in aqueous solution.[13−15] Since the first report of single-beam optical trapping, optical tweezers have been used widely for the study of molecular motors, the mechanical properties of polymer and biopolymers, colloid and mesoscopic physics, and the control of optically trapped microstructures.[16−20] The combination of microspectroscopy with optical tweezers has, thus, achieved three-dimensional spatially resolved analysis in solution.[12] Confocal laser tweezer Raman spectroscopy (LTRS) has been developed and applied for the identification and characterization of single optically trapped microparticles, red blood cells, yeast cells, and bacterial cells, and liposomal membranes.[14,15,21] Recently, LTRS has also been reported to identify the bacterial spores in aqueous solution, in which bacterial spores are discriminated from nonbiological particles, such as polystyrene spheres, on the basis of Raman signature.[22]

In this paper, we report on the rapid identification of single bacterial cells among six species in aqueous solution with confocal LTRS techniques. Previous Raman studies of microorganism identification involved deposition of bacterial cells onto substrates or solid media.[8,10] Due to the weak nature of Raman scattering, the strong background or fluorescence coming from the substrates (such as quartz or glass slips) and media seriously affects the signal-to-noise ratio and, thus, may affect the correctness of the identification. Another disadvantage of those reported studies is that they use a visible laser as the Raman excitation source,[10,22] which usually produces obvious photodamage to biological cells. The combination of optical trapping with Raman spectroscopy in this work allows capturing an individual moving bacterium in the focus of the laser beam and levitating the captured cell well above the cover substrate in the aqueous solution. This maximizes the collection of Raman scattering signal from the cell and minimizes the unwanted background from the cover plate and the environment. Therefore, the signal-to-noise ratio of the detected single cell spectrum is effectively increased. In our work, a near-infrared laser beam at 790 nm is used for both optical trapping and Raman excitation, and the photodamage is well-reduced due to the low absorption in NIR wavelength.[23]

Table 1. Bacterial Species Used in Bacterial Discrimination Studies

ID	strain
A	*Bacillus cereus*
B	*Enterobacter aerogenes*
C	*Escherichia coli*
D	*Streptococcus pyrogenes*
E	*Enterococcus faecalis*
F	*Streptococcus salivarius*

In our experiments, six bacterial species were used to demonstrate the capability of confocal LTRS in the spectroscopic identification and discrimination of single bacterial cells between various species and diverse growth phases. Since the molecular composition of bacterial cultures changes in different growth phases (i.e., lag, log, stationary, and decline phases), which may affect the Raman spectroscopic features for identification, we start the discrimination of bacterial species from synchronized cell cultures at log phase using the multivariant analysis technique of principle component analysis (PCA), then we study the spectroscopic discrimination of bacterial species for unsynchronized cell cultures at the stationary phase with the multivariant analysis techniques of PCA and hierarchical cluster analysis (HCA). Finally, we study the classification of the bacterial species for the unsynchronized cells taken from random growth phases using a general discrimination analysis (GDA) method.

MATERIALS AND METHODS

Bacterial Strains and Sample Preparation. Six bacterial species, listed in Table 1, were used in this study. For the preparation of bacterial cultures, each species was streaked onto an LB plate (containing 10 g of tryptone, 5 g of yeast extract, 10 g of NaCl, and 1.5% agar/L) from the glycerol stock. These plates were then incubated at 37 °C overnight. Single colonies from the incubated plates were transferred to 3.0 mL of LB liquid media (containing no agar) and incubated at 37 °C for 16 h to obtain the initial bacterial cultures. Then 200 μL portions of the initial cultures were transferred to each of 15 tubes (12 × 75 mm Falcon polystyrene round-bottom tube) that contained the same amount of fresh LB liquid medium (3 mL) and incubated under the same conditions (37 °C with shaking at 150 rpm) with a shaker. At every 20 min after incubation, one tube of culture was taken from the incubator for optical density (OD_{600}) measurement (UV 1201 spectrophotometer, Shimadzu). Bacterial cultures at different time points (Figure 1a, I, II, III, IV and V) on the growth curve were used for Raman measurement.

Synchronization. Synchronous cultures, which have uniform cell size/weight, were prepared by selecting the smallest cells from exponentially growing cultures using velocity sedimentation in sucrose gradients. Sucrose gradients (containing sucrose with a concentration range from 5 to 12%) were established in 12-mL

(12) Bridges, T. E.; Houlne, M. P.; Harris, J. M. *Anal. Chem.* **2004**, *76*, 576−584.
(13) Ajito, K.; Torimitsu, K. *TRAC, Trends Anal. Chem.* **2001**, *20*, 255−262.
(14) Xie, C.; Dinno, M. A.; Li, Y. Q. *Opt. Lett.* **2002**, *27*, 249−251.
(15) Xie, C.; Li, Y. Q. *J. Appl. Phys.* **2003**, *93*, 2982−2986.
(16) Ashkin, A.; Dziedzic, J. M.; Bjorkholm, J. E.; Chu, S. *Opt. Lett.* **1986**, *11*, 288−290.
(17) Mehta, A. D.; Rief, M.; Spudich, J. A.; Smith, D. A.; Simmons, R. M. *Science* **1999**, 283, 1689−1695.
(18) Bustamante, C.; Bryant, Z.; Smith, S. B. *Nature* **2003**, *421*, 423−427.
(19) Grier, D. G. *Nature* **2003**, *424*, 810−816.
(20) Neuman, K. C.; Block, S. M. *Rev. Sci. Instrum.* **2004**, *75*, 2787−2809.
(21) Sanderson, J. M.; Ward, A. D. *Chem. Commun.* **2004**, *7*, 1120−1121.
(22) Chan, J. W.; Esposiko, A. P.; Talley, C. E.; Hollars, C. W.; Lane, S. M.; Huser, T. *Anal. Chem.* **2004**, *76*, 599−603.
(23) Neuman, K. C.; Chadd, E. H.; Liou, G. F.; Bergman, K.; Block, S. M. *Biophys. J.* **1999**, *77*, 2856−2863.

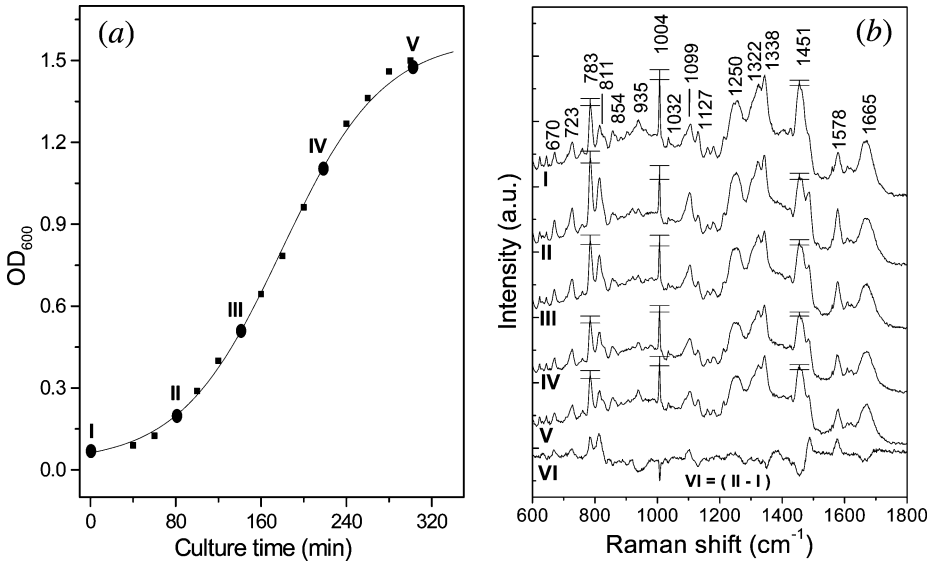

Figure 1. (a) The growth behavior of *E. coli* bacteria and (b) the averaged Raman spectra at different OD_{600} values. The curve VI is the difference spectrum between curves II and I.

volumes in 16 × 104 mm Nalgene high-speed polycarbonate tubes.[24,25] The gradient contained 1% KCl as an electrolyte. The bacterial cells were first concentrated by centrifugation for 5 min at ~4000*g* to obtain a pellet and then resuspended in 300 μL of a 2.5% sucrose solution. Then the 200-μL suspension was layered upon the gradient, spanning at 2500 rpm (~1000*g*) for 10 min in a swinging-bucket centrifuge (Sorvall centrifuge, RC2-B; rotor HB-4). After the centrifugation, the cells formed a visible band about 1.0 to 1.5 cm in width from a depth of about 1 cm below the meniscus. The top layer of the band contained the smallest size, almost uniform bacterial cells. About 100 μL of the cell suspension was removed from the top of the band and resuspended in 2 mL of the fresh LB medium, which was stored in a refrigerator at 4 °C for the following Raman measurements.

Confocal Laser Tweezers Raman Spectroscopy. The experimental setup was similar to the previous report.[15] A circularized beam from a diode laser (TIGER, Sacher Lasetechnik, Germany) at 790 nm was spatially filtered and then introduced into an inverted microscope (Nikon TE2000, Marietta, GA) equipped with an objective (100×; N.A., 1.30) to form a single-beam optical trap. The same laser beam was also used as the Raman excitation source. The Raman scattering light from an optically trapped cell (levitated ~10 μm above the quartz plate) was collected with the same objective. A 100-μm pinhole was used as an aperture to reject most of the off-focus scattering light, and a holographic notch filter was used to reject the residual excitation light. The spatially and spectrally filtered scattering light was then focused onto the entrance slit of a spectrograph equipped with a liquid nitrogen-cooled charge-coupled detector (Symphony, Jobin Yvon, Edison, NJ). The Raman spectrum was collected from 500 to 2100 cm^{-1} with a spectral resolution of ~6 cm^{-1}. For each species, the Raman spectra of 12 bacteria at each growth phase (determined by measuring the OD_{600} value) and 32 synchronized bacteria were acquired. The measurement on an individual cell was performed with an integration time of 30 s and an excitation power of 100 mW on the sample. The background spectrum was collected at the same conditions without the cell in the trap. To examine potential photodamage to an individual bacterial cell, Raman spectra were continuously recorded, and no obvious spectral change was observed within 5 min.

Spectral Preprocessing. Following the spectral acquisition, the background spectrum originating from the surrounding medium, cover plate, and other optical elements was first subtracted from each cell spectrum. The resultant spectrum was calibrated with the spectral response function of the instrument. A weak baseline was still observed after the subtraction of the background, which might result from the presence of fluorescence coming from either the trapped bacteria or the medium. To eliminate the baseline effect in the successive species discrimination, the first derivative of each Raman spectrum was taken. The derivative spectrum was then normalized to the total area, and the spectral range was reduced to highlight the fingerprint region (600−1800 cm^{-1}) for multivariate analysis.

Multivariate Analysis. The Raman spectra of single bacterial cells were analyzed using PCA, HCA, and GDA. The multivariate analysis codes and preprocessing were implemented using Matlab 6.5 software package (The Mathworks Inc., Natick, MA). The PCA and the HCA algorithms used in the analysis were obtained from the multivariate analysis toolbox PLS-toolbox (Eigenvector Research Inc., Manson, WA). The GDA algorithm was obtained from Statistical Pattern Recognition Toolbox for Matlab (Czech Technical University). The PCA was performed on all the sampled cells to reduce the dimensionality of the data set. The HCA was performed on the four PC scores, which accounts for 90% variation in the data set, obtained for each spectrum (at stationary phase) by using Ward's clustering algorithm and the squared Euclidean distance measure to generate a dendrogram. The GDA was performed in cases when within-group variance was high and between-group variance was low so as to get the better differentiation. The GDA is a kernelized version of the linear discriminant analysis. It produces the kernel data projection which increases

(24) Kubitschek, H. E.; Bendigkeit, H. E.; Loken, M. R. *Proc. Natl. Acad. Sci. U.S.A.* **1967**, *57*, 1611−1617.
(25) Kubitschek, H. E. *J. Bacteriol.* **1986**, *168*, 613−618.

class separability of the projected training data.[26] The first three PCA coefficients (or scores) were projected onto orthogonal axes as a first classifier of species identification for the synchronized populations as well as for the cells cultured to the stationary phase. For the identification of unsynchronized cells, PCA analysis was first conducted to reduce the data set, and then further analysis was conducted using the GDA algorithm with the first ten PCA scores for training.[26]

RESULTS AND DISCUSSION

Growth Curve and Raman Spectra of *Escherichia coli* Bacteria in Different Growth Phases. Growth is an orderly increase in the quantity of cellular constituents, which depends on the ability of the cell to form new protoplasm from nutrients available in the environment. For a batch culture, the environments are obviously different at different growth phases. Therefore, the bacteria at different growth phases will contain different biomolecules and are expected to generate different Raman spectral signatures.[10] Figure 1 shows the growth curve of *Escherichia coli* bacteria and the averaged Raman spectra at different phases. The bacterial growth was monitored by measuring the optical density at 600 nm. At each time point, Raman spectra of 12 randomly selected individual bacteria were acquired and averaged. Tentative assignments of the typical Raman bands are summarized in Table 2. The standard deviations of the Raman intensities at three bands (783, 1004, and 1451 cm^{-1}) were calculated and specified on the spectra. The averaged Raman spectra at different time points revealed that the spectra of bacterial cells from different growth phases were different. In Figure 1b, curve VI is the difference spectrum obtained by subtracting the averaged spectrum at point I (on growth curve) from that at point II. From the difference spectrum, it can be seen that as the bacterial cells enter the log phase (II) from the lag phase (I), the nucleic acid bands (783, 811, 1099, and 1578 cm^{-1}) are increased. This may reflect active metabolic activities involving DNA and RNA synthesis. Meanwhile, the variance in nucleic acid band 783 cm^{-1} and protein bands, such as 1004 cm^{-1}, among the individual cells is increased. This may reflect bacterial cells at log phase being in rapid division and so as in various cell cycle states. As the cell population enters the stationary phase (V), both the metabolic activities of individual cells and cell division slow. The decreases in nucleic acid bands and in spectral variance

Table 2. The Attentive Assignment of the Raman Bands[27−30]

peak position (cm^{-1})	assignment[a]	ref
670	T, G	27
723	A	27
783	C, T/DNA: O−P−O⁻	27
811	lipids: O−P−O⁻	27
854	Tyr	27
935	p: C−C bk	27
1004	Phe	27
1032	Phe	27
1099	DNA: O−P−O⁻	27, 28
1127	p: C−N, C−C str	27, 28
1250	amide III	28
1322	G/p: −CH def	27
1338	A, G/p: −CH def	27, 29
1451	lipid/p: −CH def	27, 29
1578	A, G	27, 29
1607	Phe, Tyr	27, 28
1665	amide I	27, 30

[a] Abbreviations: A, adenine; G, guanine; T, thymine; C, cytosine; Tyr, tyrosine; Phe, phenylalanine; p, protein; def, deformation; bk, backbone; str, stretching.

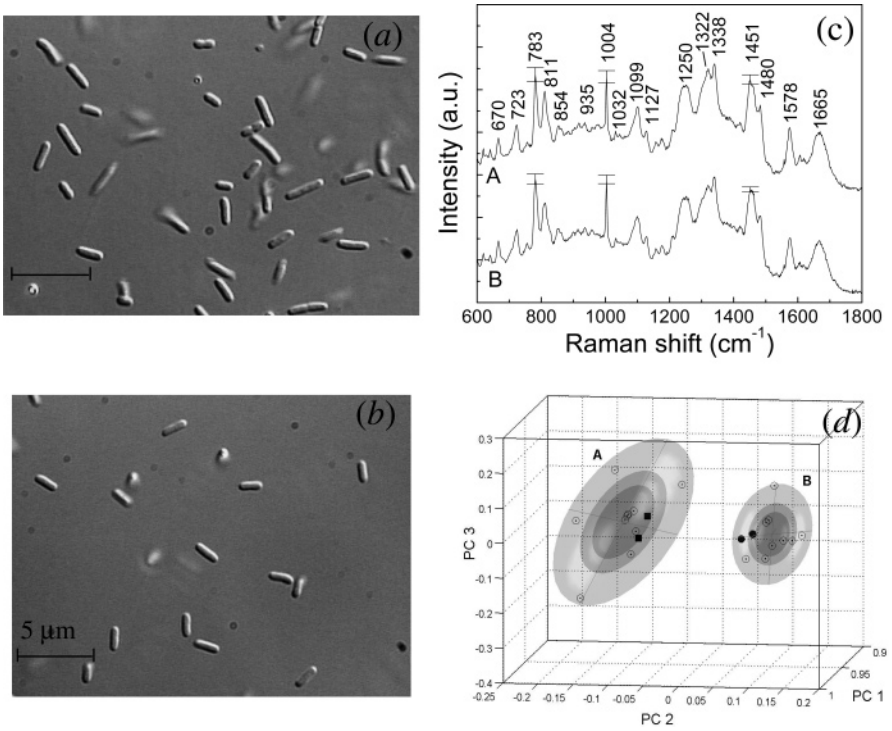

Figure 2. The images of *E. coli* bacteria (a) before and (b) after synchronization at log phase (III); (c) the averaged Raman spectra of *E. coli*, A, before synchronization; B, after synchronization; (d) the projection analysis of training sets (10 bacteria) and testing set (2 bacteria) of *E. coli* bacteria with PCA.

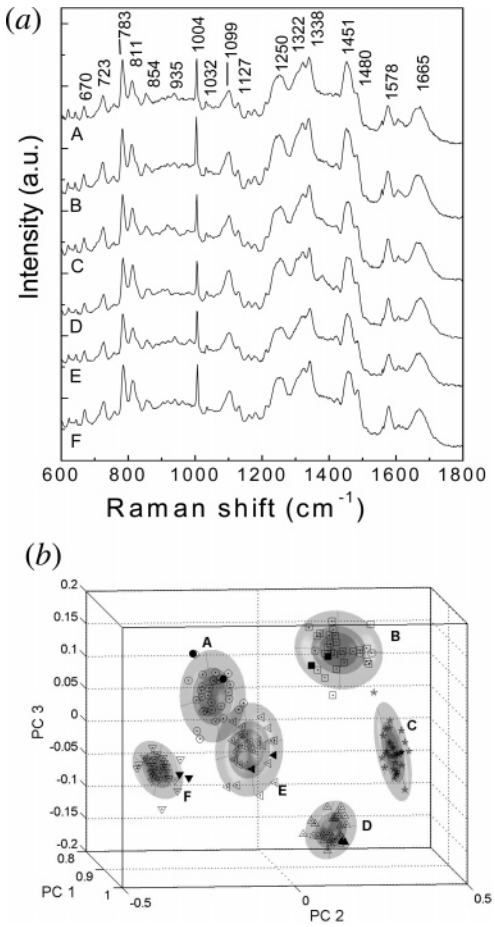

Figure 3. (a) The averaged Raman spectra of six species after synchronization and (b) projection analysis of the training (30 bacteria) and testing (2 bacteria) sets of six species after synchronization (at log phase) with PCA. The open scatter symbols are for training bacteria, and the filled symbol are for the testing bacteria.

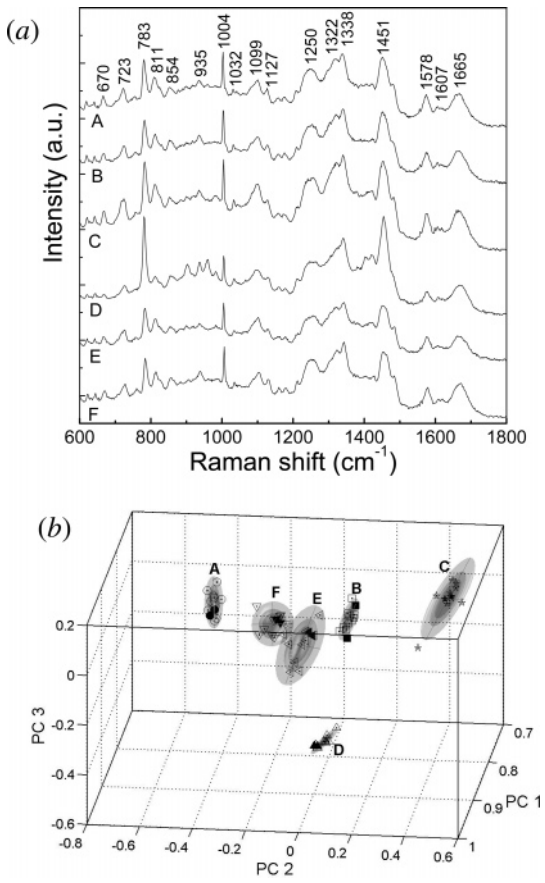

Figure 4. (a) Averaged Raman spectroscopy of six species at stationary phase and (b) the projection analysis of training (10 bacteria) and test (2 bacteria) sets with PCA.

observed in Figure 1b may reflect this effect. We also measured the growth curves of the other five species and observed similar changes in different growth phases due to the change in cellular composition. This may affect the effectiveness of the Raman spectra method for the identification of bacterial species. To reduce the effect of cellular growth, we first studied the discrimination of different bacterial species after synchronization.

Raman Spectra and Multivariate Discrimination of Synchronized Bacterial Cultures. In the batch culture, the distribution of cell size and growth cycle in a population is random. Theoretically, the smallest cells in a bacterial population are those that have just completed the process of cell division. We intended to select by velocity sedimentation those cells that had just completed the process of binary fission. In the synchronized population, the cell size is uniform, and most bacteria are at the same physiological stage, which should generate more repeatable Raman spectra for species identification. We chose the culture at log phase (point III) for synchronization. Figure 2a shows the image of the unsynchronized *E. coli* bacteria (control group), and Figure 2b shows the synchronized population. It can be seen that in the control group, the cell size is randomly distributed among individual cells. For example, the length of the largest cell is nearly twice of that of the shortest cell, and some cells have not been completely separated yet. After synchronization (Figure 2b), the size of the cells taken from the top of the centrifuged band is smaller and more uniform, which is expected to produce more consistent Raman spectra. Figure 2c shows the averaged Raman spectra of the unsynchronized and synchronized populations. The Raman intensities at three bands (783, 1004, and 1451 cm^{-1}) were measured for individual cells, and the standard deviations were calculated and specified on the spectra. The results show that the synchronized bacteria have less variance in single cell spectra, which therefore will yield more accurate discrimination. We also analyzed the variations in single-cell Raman spectra in the two populations with PCA, as shown in Figure 2d. The outermost gray ellipsoids represent 90% confidence intervals for the two clusters. Larger ellipsoids indicate greater scatter in the clusters. The graph demonstrates that synchronization effectively reduces the variance among the population, which will offer greater benefit for Raman identification of different species. It should be noted that the separation of synchronized and unsynchronized clusters in Figure 2d is due to the very small percentage of finding the smallest cells that are right after the binary division in an unsynchronized batch culture. Therefore, with the limited number of cells (10 cells for each cluster in this experiment), the synchronized and unsynchronized clusters are separated in principal component space. However, if a large number of clusters were measured in the control group, the synchronized cluster would be embedded in cluster A.

(26) Baudat, G.; Anouar, F. *Neutral Comput.* **2000**, *12*, 2385−2404.

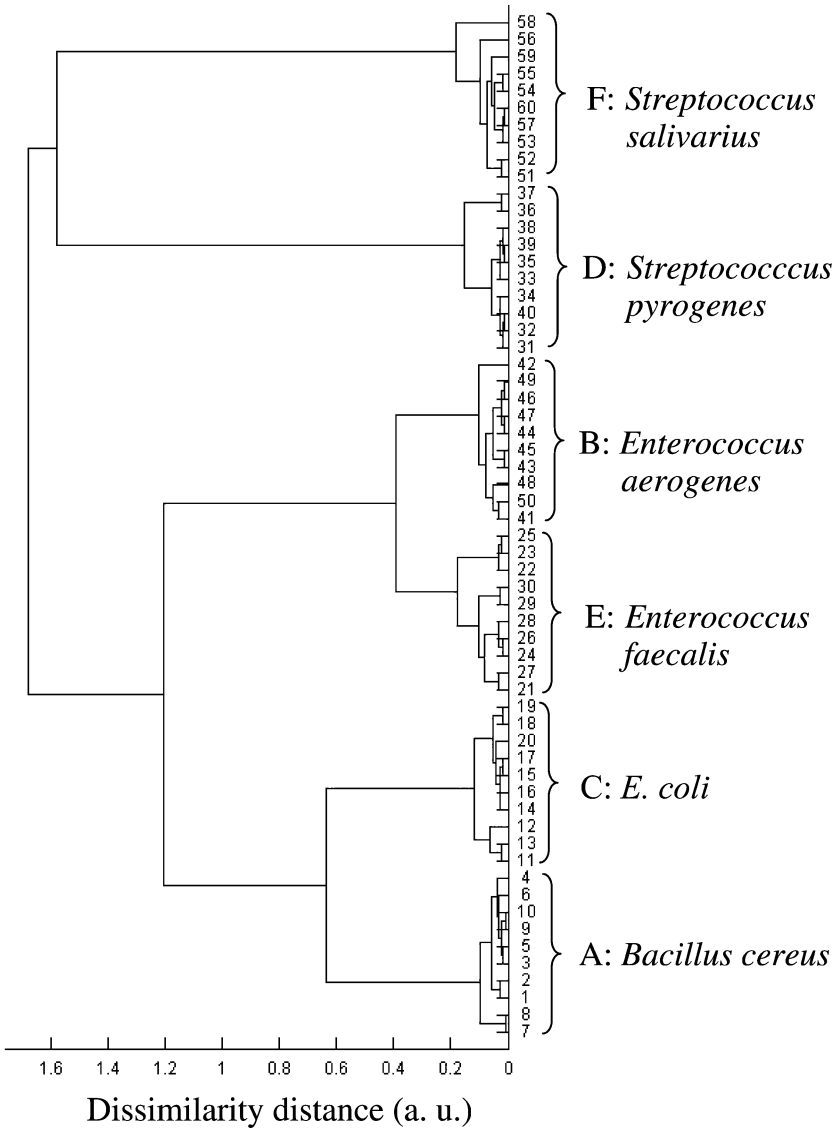

Figure 5. Dendrogram from hierarchical cluster analysis of Raman spectra of six species at stationary phase. The dendrogram was generated from the four PC scores by using Ward's clustering algorithm and the squared Euclidean distance.

Figure 3 depicts the averaged Raman spectra of six species and the PCA result after synchronization. For each species, 32 cells were randomly chosen for Raman measurements. These spectral profiles show visual similarity as well as differences. The spectral similarity lies in that they all contain common Raman bands, such as nucleic acids (783, 811, 1099, and 1578 cm^{-1}), protein (1004, 1250, and 1665 cm^{-1}), lipid (1451 cm^{-1}), carbohydrates, etc. The spectral difference between different species lies in that their relative intensities at different positions are different (Figure 3a). For example, the ratio of the Raman intensity at 783 cm^{-1} (C, T, DNA: $O-P-O^-$) to that at 1004 cm^{-1} (Phe) for curve B (*Enterobacter aerogenes*) is ~0.85, while the ratio for the other curves is close to 1. This spectral difference indicates that the composition and concentration of molecular components are slightly different for different bacterial species. This intrinsic difference in biomolecular composition and concentration for different bacterial species will cause the clusters to be separated from each other. Figure 3b shows the scatter plots of the Raman spectra for all six species projected into a three-dimensional subspace using principal component scores PC1, PC2, and PC3. For each species, 30 bacterial spectra were used as training sets to compute the PCA model, the location, and the size of ellipsoids. Two bacterial spectra per species were used for testing the correctness of the model. The outermost gray ellipsoids represent the 90% confidence interval for each of the six clusters. Figure 3b shows that the 180 single-cell spectra are clearly clustered into six distinct groups, and 12 testing spectra are located in the correct groups. This means that these six bacterial species can be well-identified and discriminated if the synchronized cultures are used. Although clusters A and E appear partially overlapped in Figure 3b, they can be clearly separated when the plot is rotated from a different angle in a 3-D graph.

Raman Spectra and Discrimination of Unsynchronized Cultures in Stationary Phases. Bacterial growth depends on nutrition, temperature, humidity, pH, etc. In natural environments, most bacteria lie in a stationary state. Therefore, testing the effectiveness of the LTRS method for the discrimination of bacteria in stationary phase is significant. Figure 4 shows the averaged Raman spectra and PCA results of the six species of bacteria cultured to stationary phase. Although the spectra of these species

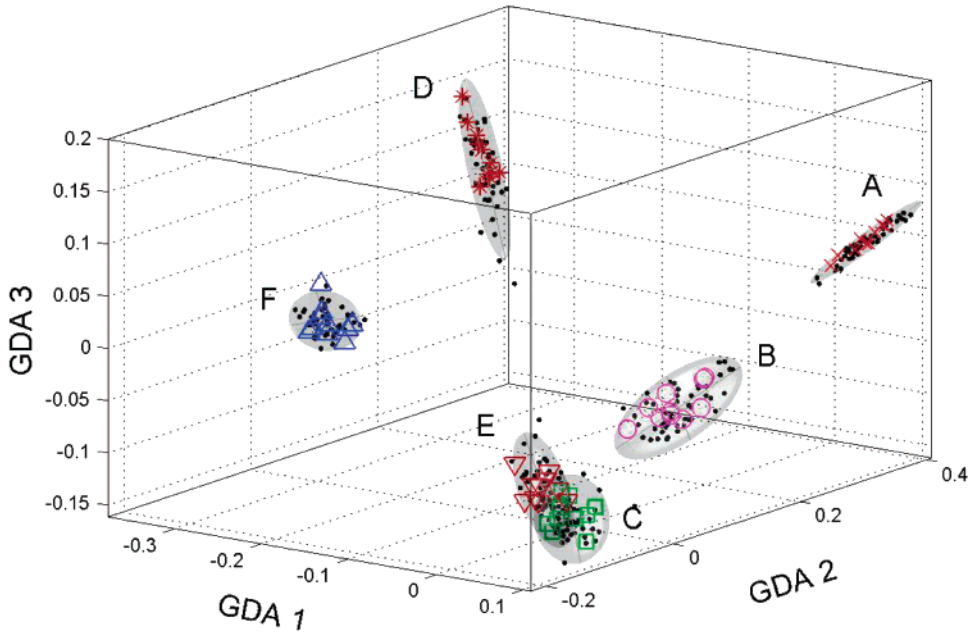

Figure 6. The projection analysis of the training sets of six species with GDA. For every species, it contains 50 training sets and every 10 sets derived from different OD_{600} values.

show visual similarity (Figure 4a), they are clearly separated in the three-dimensional space of the first three PC axes, shown in Figure 4b. In this experiment, Raman spectra of 12 individual cells per species were recorded and processed for averaged spectra. Then 10 individual spectra for each species (total 60 spectra as training set) were used for computing the PCA model, ellipsoid location, and shape. The remaining two spectra were used for testing. The outermost ellipsoids represent 90% confidence intervals for the clusters. In PCA projection, the first loading spectrum (PC1) is the least-squares regression fit of the original training data set, and it closes to the average of the original mixture spectra. The second loading spectrum (PC2) accounts for the most variance in the training data set after all mixture spectra have been made orthogonal to PC1. In Figure 4b, the six species are separated by PC2, except for cluster D, which can be separated from the other five species by the third loading spectrum (PC3). From the projection analysis, it can be seen that the six bacterial species can be well-discriminated from the unsynchronized cultures in stationary phases, although the clusters for *Enterococcus faecalis* (E) and *Streptococcus salivarius* (F) have some extent overlap (~5% at 90% confidence interval).

HCA is another nonsupervised method for obtaining information about the dissimilarity between spectra of different species. Figure 5 shows the dendrogram resulting from HCA performed on a total of 60 Raman spectra (10 for each species) of six unsynchronized cultures at stationary phase. The first four PCA scores were used as the input parameters, which account for 90% of the variation in the data set. The dendrogram was generated using Ward's clustering algorithm and the squared Euclidean distance. In Figure 5, the vertical axis represents the labeling of the 60 cells, and the horizontal axis represents the dissimilarity distance between two cells or clusters. Apparently, the 60 spectra (or cells) formed six separated clusters, one per species. The complete separation in the dendrogram was different from the cluster separation shown in Figure 4b. This is because in the HCA analysis method, the first four PC scores were used to calculate the squared Euclidean distances between different spectra, whereas in the PCA analysis, slight overlap was observed between the two clusters (E and F) because only the first three PC scores were used for projection.

General Discriminant Analysis of Unsynchronized Cultures from Random Growth Phase. We also tested the potential of Raman spectroscopy to discriminate the six species from random growth phases with the PCA method. For this purpose, we collected the Raman spectra for 12 cells at each point on the growth curve, with five points (total 60 cells) for each species. Then 10 cells from each of the five points were used to create a training set of 50 cells, and 2 cells from each point were used to create a training set of 10 cells. These were combined for all six species, giving a total of 300 cells for training and 60 cells for testing. Due to the effect of the growth phase, the within-group variance is too large to be identified simply by the PCA method; thus, GDA was used to alter the scores to maximize the between-group difference in spectral information and to minimize the within-group variation. By sending the first 10 principal components (from PCA) of the training sets to the GDA algorithm, a model was created. The altered scores (GDA scores) for the training data were used to create an ellipsoid (using mahalanobis distances) for each species. The model was applied to the testing cells, and they were projected into the subspace created by the training data. Figure 6 shows that six species had all of their testing cells located inside the correct cluster. The *E. faecalis* (E) and *E. coli* (C) have some level of overlap; the other four species were well-classified.

Compared with the other well-documented methods for bacterial discrimination,[5,6] confocal Raman tweezers is a nondestructive spectroscopic technique for microbial analysis at the single-cell level. We explored the use of confocal Raman tweezers in discriminating the six species under different physiological states. For a single species, due to the growth effect, the Raman spectra at different phases are changed. At the exponential phase (point II in Figure 1), the characteristic band intensities of RNA (723,

783, and 1578 cm^{-1}) are higher than those at the stationary phase (point V), which is consistent with the other group's report.[10,31] The within-species difference due to the growth phase affects the effectiveness of the Raman spectral method for bacterial identification. To reduce the within-group scatter, synchronized cultures prepared by velocity sedimentation are the good choice. The synchronized cells generated uniform Raman spectra so that different bacterial species can be well discriminated with the PCA analysis method.

For unsynchronized cultures, growing the cells to stationary phase would help the identification, and both the PCA and HCA analysis methods work well. The confocal Raman tweezers method requires minimal sample preparation so that the entire detection time is substantially reduced. With the nonlinear multivariable analytical method, such as GDA, six species in our study can be classified without requiring the strict standardization of the physiological state. Except for the two training sets (E and C), most of the cells are classified as the separated group. A native bacterial sample taken from the natural environment needs to be tested in the future. Associated biochemical and biomolecular methods are required to be done at the same time to confirm the effectiveness of the Raman spectral method. Genotype information should also be included to confirm the consistency of the phenotype Raman spectra analytical method so that the Raman tweezers method has even broader applications.

(27) Notingher, I.; Verrier, S.; Haque, S.; Polak, J. M.; Hench, L. L. *Biopolymers* **2004**, *72*, 230−240.

(28) Pupples, G. J.; de Mul, F. F. M.; Otto, C.; Greve, J.; Robert-Nicoud, M.; Arndt-Jovin, D. J.; Jovin, T. M. *Nature* **1990**, *347*, 301−303.

(29) Nijssen, A.; Schut, T. C. B.; Henle, F.; Caspers, P. J.; Hayes, D. P.; Neumann, M. H. A.; Puppels, G. J. *J. Invest. Dermatol.* **2003**, *119*, 64−69.

(30) Krafft, C.; Knetschke, T.; Siegner, A.; Funk, R. H. W.; Salzer, R. *Vib. Spectrosc.* **2003**, *32*, 75−83.

(31) Choo-Smith, L.-P.; Maquelin, K.; van Vreeswijk, T.; Bruining, H. A.; Puppels, G. J.; Ngo Thi, N. A.; Kirschner, C.; Naumann, D.; Ami, D.; Villa, A. M.; Orsini, F.; Dglia, S. M.; Lamfarraj, H.; Sockalingum, G. D.; Manfait, M.; Allough, P.; Endtz, H. P. *Appl. Environ. Microb.* **2001**, *67*, 1461−1469.

CONCLUSION

We have applied the confocal LTRS for rapid identification of single bacterial cells in aqueous solution. The moving bacteria can be held in the focus of the laser beam for Raman analysis with high sensitivity. We have demonstrated the effectiveness of the confocal LTRS in the discrimination of six species of microorganisms, either in synchronized cultures or in unsynchronized cultures in the stationary growth phase. PCA and HCA analyses of single cell Raman spectra show that individual cells can be discriminated for the synchronized cultures and unsynchronized cultures at stationary phase with very high confidence. Unsynchronized bacterial cells from random growth phases can also be classified with the help of GDA, although the single-cell spectra are relatively fluctuating among individual cells. These results show that the confocal LTRS sensor may be used for rapid environmental sensing of microbial cells in diverse aqueous media and growth conditions.

ACKNOWLEDGMENT

This work was support by the United States Army Space and Missile Defense Command through Contract No. DASG60-03-C-0091. We acknowledge Dr. Cindy Putnam-Evans for her kindness of providing synchronization instruments.

Received for review March 24, 2005. Accepted May 6, 2005.

AC0504971